Matter wave speckle observed in an out-of-equilibrium quantum fluid

Pedro E. S. Tavares[a], Amilson R. Fritsch[a], Gustavo D. Telles[a], Mahir S. Hussein[b], François Impens[c], Robin Kaiser[d], and Vanderlei S. Bagnato[a,1]

[a]Instituto de Física de São Carlos, Universidade de São Paulo, 13560-970 São Carlos, SP, Brazil; [b]Departamento de Física, Instituto Tecnológico de Aeronaútica, 12.228-900 São José dos Campos, SP, Brazil; [c]Instituto de Física, Universidade Federal do Rio de Janeiro, 21941-972 Rio de Janeiro, RJ, Brazil; and [d]Université Nice Sophia Antipolis, Institut Non-Linéaire de Nice, CNRS UMR 7335, F-06560 Valbonne, France

Contributed by Vanderlei Bagnato, October 16, 2017 (sent for review August 14, 2017; reviewed by Alexander Fetter, Nikolaos P. Proukakis, and Marlan O. Scully)

We report the results of the direct comparison of a freely expanding turbulent Bose–Einstein condensate and a propagating optical speckle pattern. We found remarkably similar statistical properties underlying the spatial propagation of both phenomena. The calculated second-order correlation together with the typical correlation length of each system is used to compare and substantiate our observations. We believe that the close analogy existing between an expanding turbulent quantum gas and a traveling optical speckle might burgeon into an exciting research field investigating disordered quantum matter.

matter–wave | speckle | quantum gas | turbulence

Coherent matter–wave systems such as a Bose–Einstein condensate (BEC) or atom lasers and atom optics are reality and relevant research fields. The spatial propagation of coherent matter waves has been an interesting topic for many theoretical (1–3) and experimental studies (4–7). On the other hand, optical speckle phenomena emerging as the interference of multiple independent wave fronts originated from a rough surface have been around for many years with ever-growing interest (8). The generalization of optical speckle to coherent matter waves is not yet well established, although it would be helpful to be able to use the solid statistical framework, developed over decades, in the atom optics. It may certainly create new perspectives and bring a broader and deeper understanding to the matter–wave community. Previously, there was some effort to investigate this topic. For instance, an atomic beam was used to generate speckle in a de Broglie wave (9). In that case, a multimode guidance was used together with a time-dependent second-order correlation function to characterize a matter–wave speckle. Also, Dall et al. (10) produced an atomic speckle by transmitting atoms through an optical waveguide when a multimode matter–wave guidance was on, in very close analogy with multimode light guiding into optical fibers. In this work, we evaluated the second-order correlation of an experimental turbulent BEC and determined its typical correlation length. The results were then properly compared with the correlation length of a computer-generated, elliptical speckle light map, propagating along the z direction, determined from its intensity correlation. We then discuss the remarkable similarities existing in between light and matter wave propagation in the presence of spatial disorder.

The experimental sequence to produce the turbulent BEC runs as follows. Standard ^{87}Rb BECs containing about $1-2\times10^5$ atoms in the $|F=2, m_F=+2>$ hyperfine state, with a small thermal fraction ($\lesssim35\%$) are produced in a cigar-shaped Quadrupole–Ioffe configuration (QUIC) magnetic trap, well into the Thomas–Fermi regime ($T\approx170\,\mathrm{nK}$, $T/T_0\approx0.47$). The measured trapping frequencies are $\omega_z=2\pi\times21.1(1)$ Hz in the symmetry axis and $\omega_r=2\pi\times188.2(3)$ Hz in the radial direction. To drive the BEC toward turbulence we superpose an additional sinusoidal (time-dependent) magnetic-field gradient, right after the BEC is produced. An anti-Helmholtz coil pair set with symmetry axis slightly tilted was compared with the QUIC trap symmetry axis ($\theta\lesssim5^\circ$). The field gradient defining the excitation amplitude ranged from 80 mG/cm to $790\,\mathrm{mG/cm}$ along the tilted axis, and a minimum of about $350\,\mathrm{mG/cm}$ is needed to drive the BECs into turbulence. The extra gradient oscillates at 189-Hz frequency for six full periods ($31.7\,\mathrm{ms}$), after which it is completely shut off. The perturbed BEC is held in the trap for an additional $35\,\mathrm{ms}$, after which it is switched off and the BEC is allowed to expand and fall. Resonant, time-of-flight (TOF) absorption images are acquired after variable time lapses in free fall. We checked that the BEC reached the turbulent state by running the following experimental tests. First, we analyze the density fluctuations appearing on the absorption images. Second, we determine the momentum distribution spectrum from the TOF images (11, 12) and check the power-law dependence, $n(k)\propto k^{-3}$, which characterizes the existence of an energy cascade, a fundamental

Significance

In recent years, significant progress concerning matter–wave creation and manipulation has been achieved. Fresnel diffraction, atom lasers, and nonlinear matter wave phenomena are just a few examples of recent interesting research topics. There have also been numerous studies related to the propagation of matter waves interacting with disordered potentials, but not as many concerning the disorder existing into the matter wave itself. In the present study, we analyze the disorder imprinted into a Bose–Einstein condensate (BEC) and its characteristic spatial evolution afterward. We performed careful analyses and traced a few analogies that led us to the conclusion that the perturbed BECs evolve very much in a speckle-like manner, in close analogy with a traveling-light (optical) speckle.

Author contributions: V.S.B. designed research; P.E.S.T., A.R.F., G.D.T., and F.I. performed research; P.E.S.T., A.R.F., G.D.T., M.S.H., F.I., and V.S.B. analyzed data; and P.E.S.T., A.R.F., G.D.T., M.S.H., F.I., R.K., and V.S.B. wrote the paper.

Reviewers: A.F., Stanford University; N.P.P., Newcastle University; and M.O.S., Texas A&M and Baylor Universities.

The authors declare no conflict of interest.

[1]To whom correspondence should be addressed. Email: vander@ifsc.usp.br.

feature of turbulence. Although the full characterization of turbulent regimes is still under investigation in our laboratory, it seems to depend on the condensed fraction, but not on the exact excitation conditions, provided that a stationary state was established.

The typical results determined from the free-fall expansion of the turbulent and the nonturbulent BECs are presented in Fig. 1, where the clouds' typical sizes are plotted as a function of the elapsed TOF. For a standard (nonturbulent) BEC, the expected aspect ratio inversion of the Thomas–Fermi radii during the free-fall expansion takes place at about $8.5\,\mathrm{ms}$ TOF, as shown in Fig. 1*A*. On the other hand, the turbulent BECs are known to expand in a self-similar manner, without ever inverting its aspect ratio, shown in Fig. 1*B*. The turbulent cloud presents a self-similar anomalous expansion with a shape and an aspect ratio nearly constant during the TOF (13, 14). Essentially, the preferential vortex line alignment along the radial direction, transverse to the symmetry axis direction, balances the radii expansion rates, keeping the aspect ratio locked during the TOF expansion (13). The rate expansions determined in both cases are $\dot{R}_y = 3.9(1)\,\mu\mathrm{m/ms}$, $\dot{R}_x = 0.47(1)\,\mu\mathrm{m/ms}$ for the standard BEC and $\dot{\tilde{R}}_y = 5.3(2)\,\mu\mathrm{m/ms}$, $\dot{\tilde{R}}_x = 1.5(1)\,\mu\mathrm{m/ms}$ for the turbulent BECs, clearly showing that the disordered matter wave expands faster than the coherent one. Fig. 1 *C* and *D* shows the expansion of a standard (nonturbulent) BEC and a turbulent BEC, respectively, for different TOF intervals. Fig. 1*D* presents the number density distribution and its characteristic modulations regularly observed in expanding turbulent BECs. These can be seen in detail only on snapshots acquired after sufficiently long TOF intervals ($\geq 25\,\mathrm{ms}$), when the optical depth lowers and the probe light passes through the atomic cloud, revealing its typical density distribution pattern. This fact forces a lower limit on the TOF to allow for the experimental study of turbulent density distribution patterns. We mention that, currently, it is not technically possible to perform studies at TOFs longer than $55\,\mathrm{ms}$ in our system.

To follow up the observations for the propagating matter wave, the propagation of light beams with and without speckle is presented in Fig. 2. A coherent elliptical Gaussian laser beam propagates in space, presenting aspect ratio inversion along the optical axis, similar to the aspect ratio inversion observed in coherent matter waves, such as a free-falling BEC. In that case, the traveling optical wave is characterized by its divergence angle, given by ref. 15: $\tan\theta_i = \lambda/\pi w_i$, where λ is the light wavelength and w_i the beam waist in the i direction. If we now consider the same elliptical beam, but with a speckle pattern on it, the divergence is quite different. The divergence angle for each direction is given by refs. 16 and 17, $\tan\theta_i = \lambda/\ell_i$, where ℓ_i is the speckle correlation length in the i direction. Actually, ℓ_i is normally expressed as d, which is the typical particle size found in the rough surface that generated the speckle pattern. For an isotropic speckle field the correlation length is equal in both directions, and thus the divergence is the same in any direction.

When dealing with light-wave propagation one has to take into account different regimes, namely the near and the far field. The near-field propagation regime takes place at short distances, compared with the Rayleigh length, and each and every domain expands as λ/ℓ_i, which is precisely the case studied here. The overall expansion is given by the sum of individual domains, and therefore the general spatial evolution takes place described based on different expansion rates, for each direction, since there are different numbers in each direction. The propagation does not present the aspect ratio inversion, which tends to unity at large distances (far field). In Fig. 2, the axial evolution of the light beam waists of a coherent Gaussian beam and a speckle beam are shown as a function of the propagation distance from the focus. We point out that both coherent and incoherent optical beams start with identical elliptical cross-sections, but evolve at distinct rates due to the presence or lack of disorder (speckle).

For the coherent beam, Fig. 2*A*, the inversion takes place after a given propagation distance away from the focus. In contrast, for the speckle field, Fig. 2*B*, the beam propagates in a nearly self-similar shape, and the cross-section along each dimension increases faster compared with the coherent beam. That happens when $\ell_i < w_i$, i.e., for a beam full of speckle grains, and presents a larger divergence angle. From Fig. 2 *A* and *B* the determined beam divergences in both cases are $\dot{w}_x = 3.964(2) \times 10^{-2}$, $\dot{w}_y = 4.8(1) \times 10^{-4}$ for the coherent Gaussian beam and $\dot{\tilde{w}}_x = 9.8(5) \times 10^{-2}$ and $\dot{\tilde{w}}_y = 1.67(6) \times 10^{-1}$ for the speckle beam, showing that the disordered light wave expands faster than the coherent one, the same as the turbulent quantum gas, presented in Fig. 1. Fig. 2 *C* and *D* shows

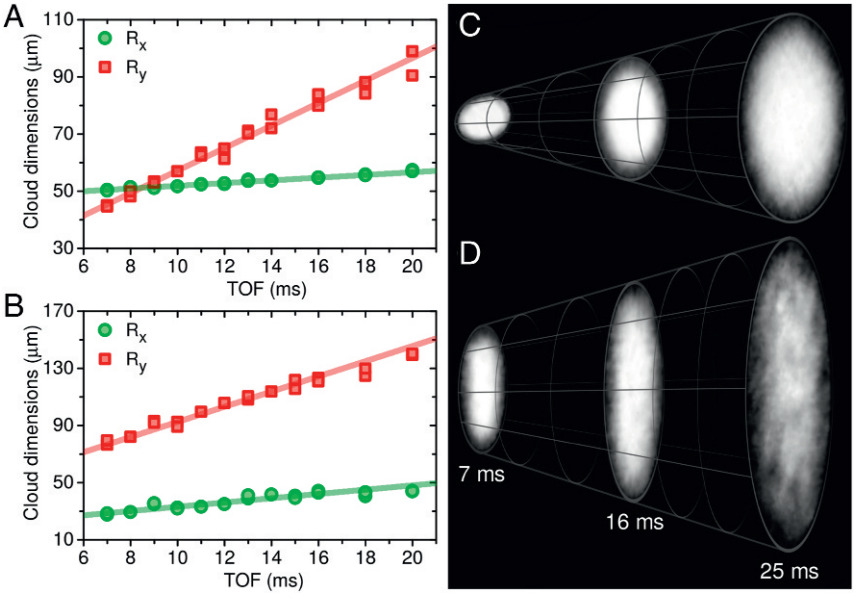

Fig. 1. BEC expansion during TOF. (*A* and *B*) The Tomas–Fermi radii, R_x and R_y, as a function of the TOF are shown for standard (*A*) and turbulent (*B*) BECs, respectively. (*C* and *D*) Three different TOF snapshots showing the expansion of standard and turbulent BECs, respectively.

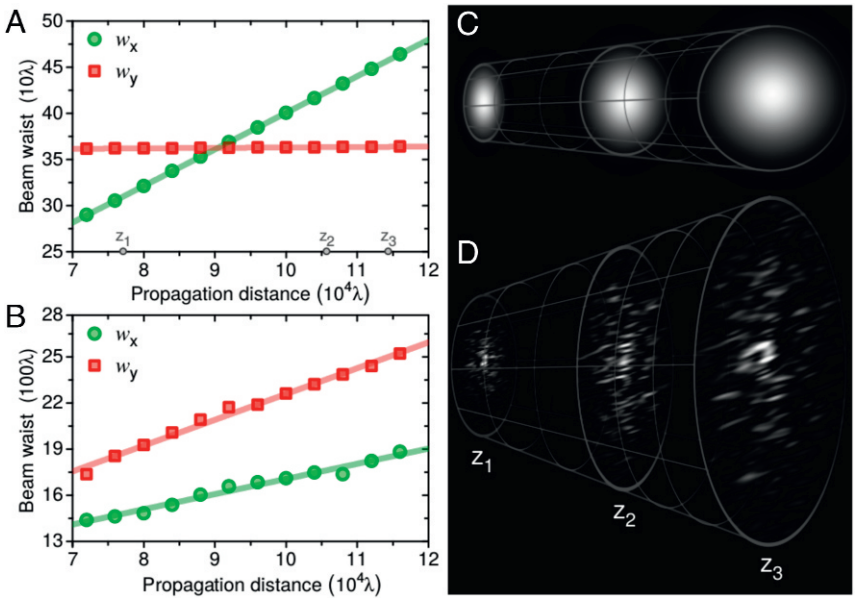

Fig. 2. Optical beam propagation. (*A* and *B*) The optical beam waists along the *x* and *y* directions, w_x and w_y, as a function of the axial distance for a coherent Gaussian beam (*A*) and the speckle beam (*B*), respectively. For the marked propagation distances z_1, z_2, and z_3, the Gaussian beam aspect ratio matches that of a standard BEC for three TOFs in Fig. 1*C*. (*C* and *D*) Sequence of three different propagation distances showing the expansion of a Gaussian beam and a speckle beam, respectively.

the propagation of the coherent Gaussian and speckle beams, respectively. Those properties presented in Figs. 1 and 2 show the equivalence between the propagating speckle light field and the expansion of the corresponding matter wave that originated from the atomic BEC strongly driven out of equilibrium. Both situations are equivalent for propagation regimes within the Rayleigh range. For much longer time propagation, both waves evolve to isotropic expansion, asymptotically. We have verified this behavior by numerical simulations for the case of a light beam with speckle.

Next, we evaluate the density–density correlation function for the expanded matter wave and compare it to that of an optical speckle, whose coherence (or the lack of it) can be expressed by the intensity–intensity correlation function. That was originally established by Hanbury-Brown and Twiss (18) in their quest for the determination of the typical sizes of astronomical objects.

The density function, $\rho(r)$, presents fluctuations due to turbulence in the sample. It is convenient to extract from $\rho(r)$ an average component and a fluctuation, a chaotic component, $\rho(r) = \langle\rho(r)\rangle + \rho_{fl}(r)$. By definition, the average of $\rho_{fl}(r)$ is zero, $\langle\rho_{fl}(r)\rangle = 0$. This property allows one to evaluate the density–density correlation function to study the turbulent BEC, given by

$$C^{(2)}(r - r') = \frac{\langle\rho(r)\,\rho(r')\rangle}{\langle\rho(r)\rangle\,\langle\rho(r')\rangle} - 1 = \frac{\langle\rho_{fl}(r)\,\rho_{fl}(r')\rangle}{\langle\rho(r)\rangle\,\langle\rho(r')\rangle}, \qquad [1]$$

and thus, according to the above definition, Eq. **1**, the correlation function for a standard BEC is null.

Concerning the fluctuations observed on the atom number density, $\rho_{fl}(r)$, the probability distribution, $P(\rho_{fl})$, is expected to be a normalized Gaussian, as a result of the central limit theorem. Thus, $P(\rho_{fl}) = N\exp[-(\rho_{fl})^2/2\sigma^2]$, where σ^2 is the variance, $\sigma^2 = \langle(\rho_{fl})^2\rangle$, and N is the normalization constant, $N = \sqrt{2/\pi\sigma^2}$. The variance is basically the correlation function at $\Delta r = r - r' = 0$. It is convenient to present our result for the correlation function normalized to the variance, such that at $\Delta r = 0$ the correlation function is unity. In this way, we define the normalized correlation function as $\widetilde{C}^{(2)}(\Delta r) = C^{(2)}(\Delta r)/C^{(2)}(0)$. Of course to calculate averages such as $\langle\rho_{fl}(r)\rho_{fl}(r')\rangle$, one needs the functional r dependence of $\rho_{fl}(r)$. Not having this at hand, we merely construct the average through sampling different values of Δr and then performing the average as $\sum_{i=1}^{M}\rho_{fl}(r_i)\rho_{fl}(r_i')/M$. The large Δr behavior of the correlation function is expected to be a Gaussian or an exponential. In our analysis to follow the exponential decay with increasing Δr was found to better represent the behavior of the data, and the correlation length can be extracted by using $\widetilde{C}^{(2)}(\ell) = 1/e$. In the following we calculate the correlation function using the measured atomic density, $\rho(r)$, obtained after expansion in TOF.

In Fig. 3*A*, we analyze the normalized correlation function $\widetilde{C}^{(2)}(\Delta r)$ of both a regular and a strongly perturbed BEC, after 30 ms of free fall. The correlation for a regular BEC is basically constant and close to zero. At short distances, $\widetilde{C}^{(2)}(\Delta r)$ for the regular BEC is greater than zero due to the small thermal fluctuations originating from the thermal atoms component of the sample. The turbulent sample shows a typical $\widetilde{C}^{(2)}(\Delta r)$ of a normalized decaying form at larger Δr, which is a result of a much shorter correlation length ($\ell_{Turb} = 8.5(2)\,\mu$m) than the sizes of the cloud ($R_x = 63(3)\,\mu$m and $R_y = 198(6)\,\mu$m) and indicates the presence of fluctuations at smaller scales. The in-trap correlation length can be extracted from the TOF correlation length by $\ell^0_{Turb} = \ell_{Turb}/\sqrt{1 + (\omega_r t)^2} \approx 1.3\xi$ (1), where t is the TOF and $\xi = 0.18\,\mu$m is the BEC healing length, which is also the typical vortex radius. The correlation length clearly indicates the dynamical randomness of the nonequilibrium BEC is entirely connected to the vortices originally created in the disturbed BEC, with further developing.

Such a behavior is very similar to a speckle light field, which motivated us to look for an underlying analogy existing between the light field and the expanding quantum degenerate gas. Indeed, the speckle field arises from a sum of complex statistically independent amplitudes bearing a random magnitude and phase (8). For this purpose, we simulated a propagating coherent Gaussian beam and

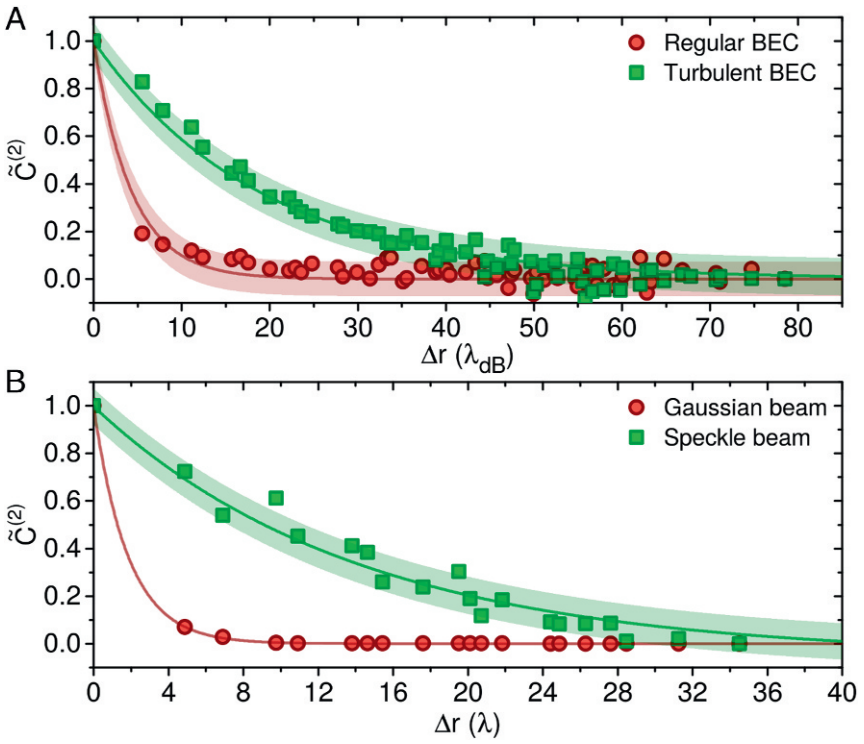

Fig. 3. Normalized correlation function, $\widetilde{C}^{(2)}(\Delta r)$. (*A*) For a regular BEC (red) and a turbulent cloud (green) as a function of the thermal de Broglie wavelength, $\lambda_{dB} = 0.45$ μm. (*B*) For the numerical simulations of a Gaussian (red) and a speckle (green) beam of light as a function of Δr, in units of λ, at a propagation distance where the Gaussian beam aspect ratio matches with the regular BEC of *A*. The $\widetilde{C}^{(2)}(\Delta r)$ for a regular BEC (Gaussian beam) is zero except for very small Δr, whereas for a turbulent cloud (speckle beam) it has an exponential decay with a correlation length of $\ell_{Turb} = 8.5(2)$ μm ($\ell_{Speckle} = 13.8(8)\lambda$). The typical dimensions are $R_x = 63(3)$ μm and $R_y = 198(6)$ μm for the BEC and $w_x = 1876\lambda$ and $w_y = 2528\lambda$ for the beam waists, showing that the correlation length is much smaller than the BEC/beam sizes. The colored regions represent the confidence bands of the exponential decay fittings.

speckle light beam and compared them with the expanding BEC and nonequilibrium BEC. In Fig. 4*B*, we present the normalized correlation function $\widetilde{C}^{(2)}(\Delta r)$ of a Gaussian and a speckle beam at a propagation distance where the Gaussian beam aspect ratio matches that of a regular BEC in Fig. 4*A*. Essentially, the same qualitative decay behavior of the correlation function is observed on the light field and on the expanding quantum gas. In Fig. 4, we present the atomic density absorption profile of an expanding turbulent cloud together with the cross-section intensity profile of a propagating speckle field, showing the similarities in the distribution of the spatial fluctuation amplitudes. An important point concerning our measurements is that they are obtained from absorption images. This corresponds to a projection of the condensate's atomic (number) density distribution onto an image plane. Despite the fact that this procedure smooths out the fluctuation amplitudes (as shown in Fig. 4), the correlation length measured after projection remains the same, as in three dimensions. This is supported by 2D simulations of an optical speckle beam and its unidimensional projection. It was observed that the effect on the correlation length, extracted from $\widetilde{C}^{(2)}(\Delta r)$, remains unaffected. In fact, the observation of a similar behavior found in the spatial evolution of such different physical systems, starting from completely different initial conditions, is truly remarkable.

The observation and study of disorder existing in matter waves freely moving in space, which can be accomplished by driving BECs to turbulence, may open up a broad research field with opportunities for understanding the inner nature of the disorder phenomena.

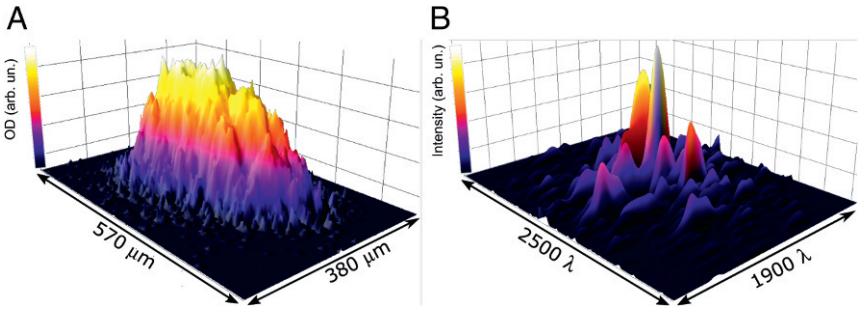

Fig. 4. Direct comparison between a turbulent BEC and an elliptical speckle beam. (*A*) Typical atom number density map of a turbulent condensate shown in units of optical depth (OD). (*B*) Light intensity map from a cross-section of a speckle beam. The integration in one of the 3Ds of the BEC results in slightly smaller amplitude for the density fluctuations.

In particular, we mention the spatial propagation of matter–waves speckle. We note that the interaction of the matter wave with random potentials created by speckle light fields has already produced very interesting results on Anderson localization (19–21). Finally, we point out that there might also be different means of nucleating disorder into quantum gases (e.g., via modulation of microscopic interactions). We do believe that similar results may be achieved once disorder in amplitude and phase is established, although we have explored it only via the turbulent regime in this work.

In conclusion, we have investigated the expansion of out-of-equilibrium (turbulent) BECs and found strong evidence that it evolves in space much like a matter–wave speckle field. This finding may well open the possibility to investigate the statistical properties of matter–waves. The speckle-like behavior observed in free-expanding quantum fluids, driven out of equilibrium, may emerge as an ideal candidate system to explore disordered patterns and the details of speckle fields traveling in three dimensions.

ACKNOWLEDGMENTS. We thank Fundacao de Amparo a Pesquisa do Estado de Sao Paulo (FAPESP) (Grant 2013/07276-1), Coordenacao de Aperfeicoamento de Pessoal de Nivel Superior (CAPES), and Conselho Nacional de Desenvolvimento Científico e Tecnológico (CNPq) (Grant PVE 400228/2014-9) for financial support. We appreciate discussions with P. Courteille and the technical assistance provided by E. Henn and G. Roati. M.S.H. also acknowledges a Senior Visiting Professorship granted by CAPES.

1. Castin Y, Dum R (1996) Bose-Einstein condensates in time dependent traps. *Phys Rev Lett* 77:5315–5319.
2. Impens F, Bordé CJ (2009) Generalized *abcd* propagation for interacting atomic clouds. *Phys Rev A* 79:043613.
3. Riou JF, et al. (2008) Theoretical tools for atom-laser-beam propagation. *Phys Rev A* 77:033630.
4. Le Coq Y, et al. (2001) Atom laser divergence. *Phys Rev Lett* 87:170403.
5. Busch T, Köhl M, Esslinger T, Mølmer K (2002) Transverse mode of an atom laser. *Phys Rev A* 65:043615.
6. Riou JF, et al. (2006) Beam quality of a nonideal atom laser. *Phys Rev Lett* 96:070404.
7. Couvert A, et al. (2008) A quasi-monomode guided atom laser from an all-optical Bose-Einstein condensate. *Europhys Lett* 83:50001.
8. Goodman JW (2007) *Speckle Phenomena in Optics: Theory and Applications* (Roberts & Company Publishers, Greenwood Village, CO).
9. Patton FS, Deponte DP, Elliott GS, Kevan SD (2006) Speckle patterns with atomic and molecular de Broglie waves. *Phys Rev Lett* 97:013202.
10. Dall RG, et al. (2011) Observation of atomic speckle and Hanbury Brown-Twiss correlations in guided matter waves. *Nat Commun* 2:291.
11. Thompson KJ, et al. (2014) Evidence of power law behavior in the momentum distribution of a turbulent trapped Bose-Einstein condensate. *Laser Phys Lett* 11:015501.
12. Tsatsos MC, et al. (2016) Quantum turbulence in trapped atomic Bose–Einstein condensates. *Phys Rep* 622:1–52.
13. Caracanhas M, Fetter AL, Baym G, Muniz SR, Bagnato VS (2013) Self-similar expansion of a turbulent Bose-Einstein condensate: A generalized hydrodynamic model. *J Low Temp Phys* 170:133–142.
14. Caracanhas M, et al. (2012) Self-similar expansion of the density profile in a turbulent Bose-Einstein condensate. *J Low Temp Phys* 166:49–58.
15. Kogelnik H, Li T (1966) Laser beams and resonators. *Proc IEEE* 54:1312–1329.
16. Giglio M, Carpineti M, Vailati A (2000) Space intensity correlations in the near field of the scattered light: A direct measurement of the density correlation function $g(r)$. *Phys Rev Lett* 85:1416–1419.
17. Goodman JW (1985) *Statistical Optics* (Wiley, New York).
18. Hanbury-Brown R, Twiss RQ (1956) Correlation between photons in two coherent beams of light. *Nature* 177:27–29.
19. Sanchez-Palencia L, et al. (2007) Anderson localization of expanding Bose-Einstein condensates in random potentials. *Phys Rev Lett* 98:210401.
20. Billy J, et al. (2008) Direct observation of Anderson localization of matter waves in a controlled disorder. *Nature* 453:891–894.
21. Roati G, et al. (2008) Anderson localization of a non-interacting Bose-Einstein condensate. *Nature* 453:895–898.